Published online 10 September 2012 *Nucleic Acids Research, 2012, Vol. 40, No. 21* ***10937–10949***
doi:10.1093/nar/gks832

Small RNA deep sequencing reveals a distinct miRNA signature released in exosomes from prion-infected neuronal cells

Shayne A. Bellingham[1,2], Bradley M. Coleman[1,2] and Andrew F. Hill[1,2,3,*]

[1]Department of Biochemistry and Molecular Biology, [2]Bio21 Molecular Science and Biotechnology Institute and [3]Mental Health Research Institute, The University of Melbourne, Parkville, Victoria 3010, Australia

Received December 8, 2011; Revised and Accepted August 9, 2012

ABSTRACT

Prion diseases are transmissible neurodegenerative disorders affecting both humans and animals. The cellular prion protein, PrP^{C}, and the abnormal infectious form, PrP^{Sc}, are found associated with exosomes, which are small 50–130 nm vesicles released from cells. Exosomes also contain microRNAs (miRNAs), a class of non-coding RNA, and have been utilized to identify miRNA signatures for diagnosis of disease. While some miRNAs are deregulated in prion-infected brain tissue, the role of miRNA in circulating exosomes released during prion disease is unknown. Here, we investigated the miRNA profile in exosomes released from prion-infected neuronal cells. We performed the first small RNA deep sequencing study of exosomes and demonstrated that neuronal exosomes contain a diverse range of RNA species including retroviral RNA repeat regions, messenger RNA fragments, transfer RNA fragments, non-coding RNA, small nuclear RNA, small nucleolar RNA, small cytoplasmic RNA, silencing RNA as well as known and novel candidate miRNA. Significantly, we show that exosomes released by prion-infected neuronal cells have increased let-7b, let-7i, miR-128a, miR-21, miR-222, miR-29b, miR-342-3p and miR-424 levels with decreased miR-146 a levels compared to non-infected exosomes. Overall, these results demonstrate that circulating exosomes released during prion infection have a distinct miRNA signature that can be utilized for diagnosis and understanding pathogenic mechanisms in prion disease.

INTRODUCTION

Prion diseases are invariably fatal, transmissible neurodegenerative disorders that include Creutzfeldt–Jakob disease (CJD); Gerstmann–Sträussler–Scheinker syndrome (GSS); fatal familial insomnia and kuru in humans, scrapie in sheep, bovine spongiform encephalopathy (BSE) in cattle and chronic wasting disease in cervids. According to the protein-only model of prion propagation, these diseases are associated with the conformational conversion of the host-encoded cellular prion protein (PrP^{C}), into an abnormal pathogenic isoform (PrP^{Sc}) by a protein-only template-directed mechanism (1). Prion diseases are characterized by a protracted asymptomatic pre-clinical period, whereby PrP^{Sc} continually propagates, prior to the rapid onset of dementia, neuronal loss, spongiform change and ultimately death [reviewed in (2)]. Effective diagnosis and treatment of prion disease is hampered by the absence of effective ante-mortem diagnostic methods. The identification of non-invasive, sensitive and specific diagnostic markers during the pre-clinical phase is of major importance.

Exosomes are small membranous vesicles, 50–130 nm in diameter, that derive from the invagination of endosomal compartments called multivesicular bodies (MVBs) to form intraluminal vesicles (ILVs). ILVs are released into the extracellular environment as exosomes when the MVB fuses with the plasma membrane (3). Several studies have identified exosomes to be released by different cell types with various functions in platelet activation, antigen presentation, immune response, cell–cell communication and spread of infectious agents (3). Previously, it has been demonstrated that PrP^{C} and PrP^{Sc} are released in association with exosomes and can transmit infection both *in vitro* and *in vivo* (4,5). Furthermore, exosomes released from prion-infected cells can initiate prion infection of cells originating from different tissues (5). This is a

*To whom correspondence should be addressed. Tel: +61 3 8344 2308; Fax: +61 3 9348 1421; Email: a.hill@unimelb.edu.au

significant observation as exosomes may mimic the spread of infectivity to peripheral tissues in the spread of neurodegenerative disease (6). Exosomes have also been shown to contain messenger RNA (mRNA) and microRNA (miRNA) that can be unidirectional and functionally transferred between cells (7,8).

miRNAs are a class of non-coding RNA (ncRNA) species of ~22 nt in length that functionally repress target mRNA by binding their 3′-untranslated regions (9). In mammals, gene regulation is achieved by mismatch base paring of mature miRNA sequence with the target mRNA allowing post-translational repression or in some cases up-regulation (10). miRNAs are involved in several biological processes, such as proliferation, development, differentiation and apoptosis (11). Since a single miRNA can potentially target hundreds of genes, aberrant miRNA expression can also initiate disease, such as cancer (12). Significantly, miRNA profiles of circulating exosomes isolated from peripheral blood (13), serum (14,15) and saliva (16) have been generated and suggest they have diagnostic potential for human disease. Indeed, the study by Skog *et al.* (15), demonstrated that glioblastoma could be diagnosed by analysing the exosomal miRNA profile in serum.

miRNA signatures have also been reported in prion-infected mice and primates (17,18). Both studies examined the miRNA profile in brain tissue of terminally prion-infected animals after clinical symptoms of disease were well established and determined a subset of miRNAs to be significantly deregulated. However, the role of miRNA deregulation in circulating exosomes during prion disease remains unknown. Therefore, we investigated whether prion-infected exosomes contain a specific miRNA signature that could also be utilized for diagnosis and increasing our understanding of cellular pathways involved in prion disease. To do this, we utilized a neuronal cell culture system that mimics pre-clinical disease by continually propagating prion infection and releasing exosomes containing prion infectivity (5). Utilizing small RNA deep sequencing, we demonstrate that exosomes released from prion-infected neuronal cells contain a variety of small RNA sequences as well as known and candidate miRNA. In particular, we report a specific miRNA signature is associated with exosomes released from prion-infected neuronal cells that can be utilized for disease diagnostics and we discuss the possible role of exosome-mediated transfer of miRNAs during prion infection and propagation.

MATERIALS AND METHODS

Reagents and antibodies

Unless specified, all reagents are from Sigma. The following antibodies and concentrations were used for western blotting: anti-PrP antibody ICSM-18 (D-Gen Limited, UK) at 1:25 000, anti-tsg101 (M-19, Santa Cruz Biotechnology) at 1:3000, anti-GM130 at 1:250, anti-Bcl-2 (BD Biosciences) at 1:1000, anti-nucleoporin (p62, BD Biosciences) at 1:1000, anti-flotillin-1 (BD Biosciences) at 1:3000, anti-mouse HRP (GE Healthcare) at 1:25 000 and anti-goat HRP (Sigma) at 1:100 000.

Cell culture and prion infection

Mouse hypothalamic neuronal (GT1-7) cell lines were maintained at 37°C in 5% CO_2 and cultured in Opti-MEM (Invitrogen), supplemented with 10% exosome-depleted heat-inactivated foetal calf serum (FCS) (Invitrogen). The M1000 prion strain was prepared from brains of terminally sick BALB/c mice infected with the mouse-adapted human Fukuoka-1 prion strain. In order to generate cells persistently infected with prions, GT1-7 cells were seeded into six-well plates (Nunc) and then incubated with 1% (w/v) normal brain homogenate or M1000 brain homogenate as previously described (5). After 5 h post-inoculation, additional Opti-MEM was added and cells were incubated for a further 3 days. Cells were then washed in phosphate buffered saline (PBS) and passaged as described. The preparation of M1000 brain homogenate is described in Supplementary Methods.

Exosome isolation

Exosomes were routinely isolated and purified from the media of uninfected or M1000 prion-infected GT1-7 cell cultures using the differential centrifugation protocol as described previously (5). Briefly, GT1-7 cells ($\sim 2 \times 10^7$ cells or $5 \times$ T175 flasks) were cultured in exosome free media (complete media containing exosome-depleted FCS) for 4 days. Culture supernatants were collected and cellular debris was removed by centrifugation at 3000*g* for 10 min. The supernatant was filtered (0.2 μm) and filtrate was centrifuged at 10 000*g* for 30 min at 4°C. The supernatant was collected and centrifuged 100 000$g_{(av)}$ to pellet exosomes. Exosome pellets were then washed in filtered PBS and re-centrifuged at 100 000$g_{(av)}$, the supernatant was removed and the final exosome pellet was re-suspended in 100 μl PBS.

Transmission electron microscopy

A 20-μl aliquot of exosomes was fixed with 1% glutaraldehyde for 30 min; 6 μl was then absorbed onto glow-discharged 300-mesh heavy-duty carbon-coated formvar Cu grids (ProSciTech, SA, Australia) for 2 min and excess blotted on filter paper (Whatman). Grids were washed twice with MilliQ water and negatively stained with 2.5% uranyl acetate. Data were collected on a Tecnai G2 F30 transmission electron microscope (FEI, Eindhoven, The Netherlands) operating at 300 kV, with defocus between 10 and 16 μm, across 15 000× to 36 000× magnification.

Total RNA isolation

Total RNA from exosomes and cultured cells were isolated using mirVana miRNA Isolation Kit (Ambion) with the use of TRIzol (Invitrogen) for organic phase separation. The amount, quality and composition of isolated RNA were analysed by BioSpec-nano (Shimadzu) for total RNA and an Agilent 2100 Bioanalyzer for total

RNA and small RNA profiles using RNA 6000 Nano and Small RNA Kits (Agilent). The isolation of total RNA, including miRNA, is described in Supplementary Methods.

Western blotting

Cells and exosomes were incubated on ice in lysis buffer (150 mM NaCl, 1% sodium deoxycholate, 1% Triton X-100, 50 mM Tris pH 7.4) containing complete protease inhibitors (Roche) and supernatants were collected to determine protein concentration by BCA assay (Pierce). One hundred micrograms of total protein was digested with proteinase K (PK, 25 μg/ml) for 1 h at 37°C and proteolysis was stopped by the addition of 4 mM phenylmethylsulfonyl fluoride. Proteins were collected by methanol precipitation, boiled in SDS–PAGE sample buffer [2% (w/v) sodium dodecyl sulphate (SDS), 10% (v/v) glycerol, 12.5 mM ethylenediaminetetraacetic acid, 2 mg bromophenol blue, 50 mM Tris pH 6.8] with 5% ß-mercaptoethanol and analysed by SDS–PAGE on NuPAGE Bis–Tris (4–12%) gradient acrylamide gels (Invitrogen). Proteins were electroblotted onto polyvinylidene difluoride (PVDF) membranes and detected by enhanced chemiluminescence (ECL) (GE Healthcare), according to the manufacturer's instructions.

miRNA profiling

The expression of miRNA in cells and exosomes was profiled using stem–loop quantitative RT-PCR (qRT-PCR) miRNA assays on TaqMan low-density array cards (TLDA) cards (Rodent Array Card A v2.0, Applied Biosystems). The cards contain assays for 375 Rodent mature miRNAs present in the Sanger miRBase v13.0. qRT-PCRs were performed with Megaplex Primers Pool A with pre-amplification according to the manufacturer's instructions. Briefly, total RNA (3 μl per sample/card) was reverse transcribed using TaqMan miRNA Reverse Transcription Kit (Applied Biosystems) with Megaplex Primers Pool A and then pre-amplified with Megaplex PreAmp Primers Pool A (Applied Biosystems). The pre-amplified cDNA was run on TLDA cards on Applied Biosystems 7900HT using the manufacturer's recommended cycling conditions. C_t values >35 were below detection limit and excluded. Data were analysed by the $\Delta\Delta C_t$ method with uninfected as the reference and snoRNA135 and snoRNA202 as the most stable endogenous controls as determined by geNorm and NormFinder algorithms using DataAssist Software v3 (Applied Biosystems). Full details of cDNA amplification are provided in Supplementary Methods.

Small RNA deep sequencing

Total RNA, containing the small RNA fraction, was converted into cDNA libraries using the SOLiD Small RNA Expression Kit (Applied Biosystems), according to manufacturer's instructions. Briefly, total RNA (3 μl per sample, ~100–250 ng small RNA) was ligated overnight with adapters 'A', reverse transcribed, RNAse H-treated and PCR amplified with unique barcode-labelled amplification primers, before size selection on 6% native polyacrylamide gels. DNA fragments between 105 and 150 bp corresponding to the small RNA population were excised, eluted and precipitated. The final DNA pellet was air dried and re-suspended in 20 μl of nuclease-free water. The size, quantity and quality of DNA in each final small RNA library were verified using DNA 1000 Kit (Agilent). Equimolar amounts for each final library were pooled at a final concentration of 41 pg/μl and used in the emulsion PCR and template bead preparation, according to the manufacturer's instructions (Applied Biosystems, SOLiD System 4.0 user guide). Barcoded template beads from all libraries were deposited on a single slide and sequenced using the SOLiD 4 Platform (Applied Biosystems). The results were obtained as colorspace FASTA files (csfasta). Primary small RNA sequencing data for all four exosomal small RNA libraries were available from the NIH short reads archive (SRA048148). The generation of small RNA libraries is explained in detail in Supplementary Methods.

Bioinformatics

Analysis of the SOLiD csfasta files was performed by miR-Intess small RNA pipeline (InteRNA Genomics B.V., The Netherlands). Briefly, the pipeline is designed to pre-process raw reads to trim and remove adapter sequences and generate high-quality reads that can be mapped to the mouse genome assembly NCBIM37 and miRBase v16 (19). Aligned reads were classified according to genomic loci annotations. Reads that aligned to intergenic or intronic regions but not to exons, repeats or structural RNAs, were used in the miRNA discovery part of miR-Intess pipeline to identify novel and candidate miRNAs following strict guidelines. Sequence reads that were classified as sense RNA (mRNA fragments) or ncRNA were further annotated by CLC Genomics Workbench (CLC Bio) to mouse genome assembly NCBIM37 and NONCODE v3 database (20), respectively. Full details of the miR-Intess small RNA pipeline are described in Supplementary Methods.

miRNA validation assays

Individual TaqMan miRNA assays (Applied Biosystems) were performed according to the manufacturer's instructions. Briefly, 5 μl of total RNA isolated from cells and exosomes was converted to cDNA using the microRNA reverse transcriptase Kit (Applied Biosystems) with 3 μl of specific miRNA assay RT primer in a reaction volume of 15 μl. cDNA was diluted and setup in quadruplicate qRT-PCRs containing 1 μl of specific TaqMan miRNA assay using the QIAgility liquid-handling robot (QIAGEN) and run on a StepOnePlus qRT-PCR instrument (Applied Biosystems) using the manufacturer's recommended cycling conditions. Data were analysed by the $\Delta\Delta C_t$ method with uninfected as the reference and snoRNA135 and snoRNA202 as endogenous controls using DataAssist Software v3 (Applied Biosystems). Full details of TaqMan miRNA assays and primers are described in Supplementary Methods.

Pathway analysis

Potential miRNA targets were identified from TargetScan, TarBase, miRecords and Ingenuity Knowledge Base using Ingenuity Pathway Analysis Software v9.0 (Ingenuity Systems). miRNA Target filter was then applied to identify experimental validated targets and analysed for known interactions with the prion gene and protein.

Statistical analysis

All data represent the mean ± SEM and statistical Mann–Whitney *U*-tests were performed using GraphPad Prism v4 (GraphPad Software).

RESULTS

Exosomes released from prion-infected mouse hypothalamic neuronal cells contain miRNA

Cellular models of prion disease infectivity in mouse hypothalamic neuronal (GT1-7) cells have been well established (21). These cells were infected with the mouse-adapted M1000 strain (also referred to as Fukuoka-1) (22), which was derived from a patient with GSS, and is a valid model for generating infectious PrP^{Sc} as indicated by the presence of proteinase K (PK)-resistant PrP (Figure 1A). Exosomes were isolated from normal and M1000-infected GT1-7 cells using ultracentrifugation and shown to be positive for presence of PK-resistant PrP^{Sc} (Figure 1A). The purity of exosome preparations was determined by western blotting with a panel of antibodies for endosomal, plasma membrane, nuclear, Golgi and mitochondrial markers, and by transmission electron microscopy (TEM). Exosomes were enriched in tsg-101 and flotillin-1 while no detectable GM130, nucleoporin or Bcl-2 was present indicating that our exosome preparations were enriched in proteins of endosomal origin and that no contaminating nucleus, Golgi, mitochondrial and apoptotic membranes were present (Figure 1B). TEM demonstrated that exosomes isolated from GT1-7 cells were composed of extracellular vesicles of ~100 nm in size and consistent with the known morphology (Figure 1C).

Exosomal RNA has been isolated from exosomes derived from mast cells and cancer cells (7,14,23); however, the presence of miRNA and mRNA in neuronal cell-derived exosomes has yet to be determined. Using our exosomes from uninfected and infected GT1-7 cells, we isolated total RNA including the small RNA fraction. The quality and quantity of the isolated RNA were determined using an Agilent Bioanalyzer (Figure 1D). Total RNA bioanalyser profiles indicated that neuronal cell-derived exosomes lack detectable amounts of 18S and 28S ribosomal RNA (rRNA) species in agreement with exosomes derived from other cell lines (7,14,23). Small RNA bioanalyser profiles between cells and exosomes indicated that neuronal cell-derived exosomes are enriched in transfer RNA (tRNA) species and contain small RNA between 4 and 40 nt in length consistent with miRNA. This is the first demonstration to our knowledge that neuronal cell-derived exosomes contain both mRNA and miRNA species.

Prion-infected exosomes contain a subset of dysregulated miRNA

Utilizing the isolated miRNA from uninfected and prion-infected cells and their corresponding exosomes, we profiled the miRNA using TLDA cards that can detect 375 known miRNA species. We detected 194 (~52%) miRNAs in GT1-7 cells with 189 of these detected in both uninfected and prion-infected cells (Figure 2A and Supplementary Table S1). Five miRNAs were exclusively detected at low levels in either uninfected or infected cells. miR-210 (Av $C_t > 30$) and miR-294 (Av $C_t > 34$) were only detected in uninfected cells (Figure 2A and Supplementary Table S1), while miR-20 a, miR-451 (Av $C_t > 33$) and miR-302 b (Av $C_t > 32$) were only detected in infected cells (Figure 2A and Supplementary Table S1). In exosome preparations isolated from the same cells, we detected 157 (~42%) specific miRNAs in both uninfected and prion-infected exosomes (Figure 2B and Supplementary Table S2). Relative quantitation of the 189 miRNAs detected in both uninfected and prion-infected cells identified 12 miRNAs that were >2-fold up-regulated and 5 miRNAs that were <2-fold down-regulated upon prion infection in GT1-7 cells (Figure 2C). While, relative quantitation of 157 miRNAs detected in both uninfected and prion-infected exosomes identified several miRNAs that were differentially expressed. miR-182, miR-29 b, miR-296-3 p and miR-424 were >2-fold up-regulated and miR-126-3 p, miR-134, miR-146 a, miR-186, miR-188-5 p, miR-193 b, miR-222 and miR-380-5 p were <2-fold down-regulated in exosomes released from prion-infected neuronal cells (Figure 2D). Notably, miR-146a and miR-222 were <2-fold down-regulated upon prion infection in both cells and exosomes (Figure 2C and D). Overall, these results suggest that the miRNA profile between cells and exosomes is differentially expressed upon prion infection and also agrees with observations that miRNA is sorted and released in exosomes by unknown mechanisms (24,25).

Exosomal small RNA deep sequencing with SOLiD platform

Next-generation sequencing technologies have been utilized to profile miRNA in several species including plants, rice, insects, chickens, rodent and human tissues (26–31). Using the miRNA fraction isolated from neuronal cell-derived exosomes for TLDA studies, we generated small RNA cDNA libraries from uninfected and prion-infected exosomes and performed, to our knowledge, the first study of small RNA deep sequencing of exosomes using the SOLiD platform. Small RNA sequencing the exosome libraries yielded raw reads that were pre-processed and trimmed to remove adapter sequences using the miR-Intess small RNA pipeline to identify high-quality reads that were considered for further analysis (Supplementary Table S3). Reads were

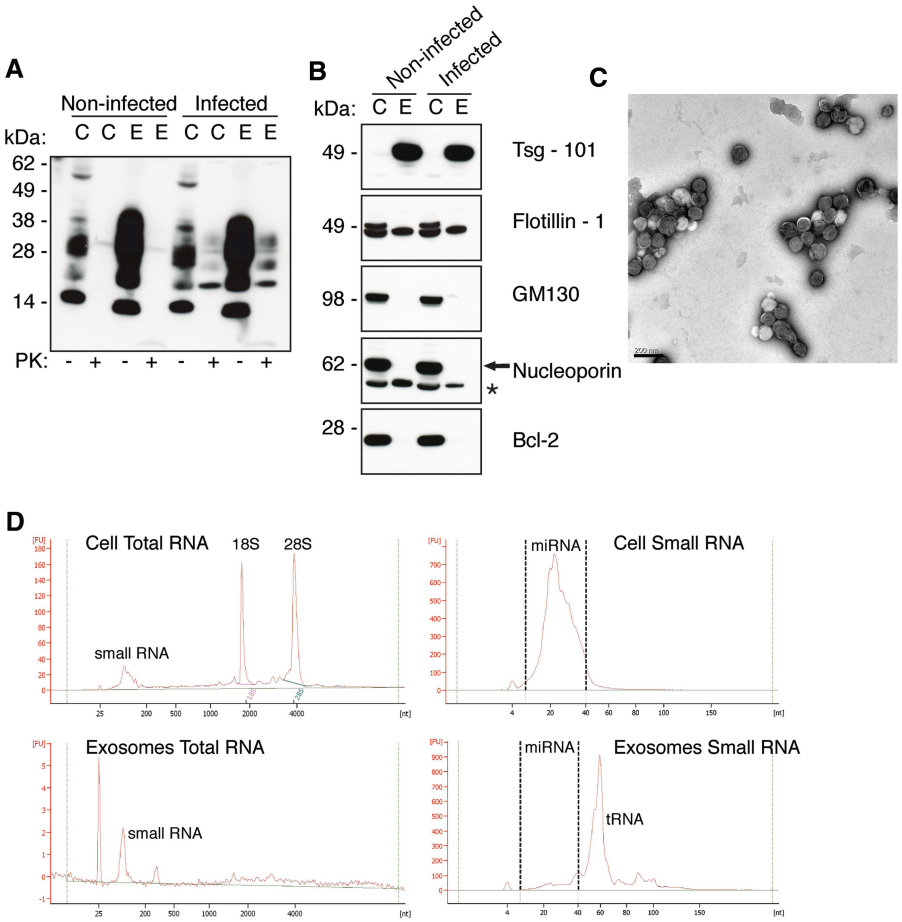

Figure 1. Exosomes isolated from prion-infected cells contain small RNA. (**A**) Western blot of PrP^{C} and PrP^{Sc} in GT1-7 cell lysates and GT1-7 exosomes. Anti-PrP antibody ICSM-18 reveals the presence of PrP in GT1-7 cell (C) lysates and GT1-7 exosome (E) lysates (40 μg total protein loaded) from both non-infected and infected samples, and following PK-digested (100 μg total protein digested with 25 μg/ml PK) PrP^{Sc} is indicated by presence PK-resistant protein in infected (C) cell lysates and exosomes (E). (**B**) Isolated exosomes were confirmed by enrichment of exosome markers tsg-101 and flotillin-1, and negative for Golgi marker GM130, nuclear marker nucleoporin and mitochondrial marker Bcl-2. Asterisks indicate non-specific band for anti-nucleoporin, p62. (**C**) Representative TEM of non-infected GT1-7 exosomes revealed homogenous populations of extracellular vesicles of ~100 nm in diameter that are characteristic of exosomes. Scale bar 200 nm. (**D**) Bioanalyser analysis of RNA isolated from cells and exosomes on the total RNA and small RNA Chips. Exosomes lack detectable 18 S and 28S rRNA bands compared to total cell RNA. Cells and exosomes both contain miRNA between 4 and 40 nt, with exosomes enriched in tRNA at ~60 nt.

subsequently mapped to identify 4 395 094 and 3 676 525 reads that matched sequences in the mouse genome and miRBase in uninfected and prion-infected exosomes, respectively (Supplementary Table S4). The composition of the exosome libraries revealed that uninfected and prion-infected exosomes contained RNA repeat regions (~50%) comprising retroviral sequences SINEs and LINEs, a very small proportion of rRNA (0.48%) consisting of mostly 5 S RNA sequences (Supplementary Figure S1A), ~33% of sequences mapped to the genome comprising mRNA fragments (Supplementary Figure S1B), ncRNA and other RNA hairpin and non-hairpin regions. The remaining (~15%) sequences were annotated to small RNA sequences derived of miRBase miRNA, candidate miRNA, tRNA, small nucleolar RNA (snoRNA), small nuclear RNA (snRNA), silencing RNA (siRNA), siRNA derived from ncRNAs and small cytoplasmic RNA (scRNA) (Figure 3 and Supplementary Table S5).

Sequence reads that mapped to ncRNAs were further annotated to the NONCODE database (20). The most abundant ncRNAs identified included 7SL RNA and Y RNA (Supplementary Figure S1C). Other ncRNA species identified to be of high abundance annotated to classes of mRNA-like long ncRNAs (Supplementary Figure S1D), piwi-interacting RNAs, long intronic ncRNAs and other non-functional annotated ncRNAs (Supplementary Figure S1E). Normalization of abundant ncRNA sequence reads suggested that no discernible difference can be seen between uninfected and prion-infected exosomes libraries (Supplementary Figure S1C–E).

miRBase annotation identified 401 known miRNAs from 12 818 small RNA reads (0.99%) in exosomes released from uninfected cells (Figure 3A), while exosomes from prion-infected cells contained 8738 small RNA reads (0.73%) that mapped to 335 known miRNAs (Figure 3B). The miR-Intess analysis pipeline also determined 20 665 small RNA reads (1.58%) that annotated to 756 candidate novel miRNAs in uninfected exosomes (Figure 3A) and 16 094 small RNA reads (1.34%) that annotated to 739 candidate novel miRNAs

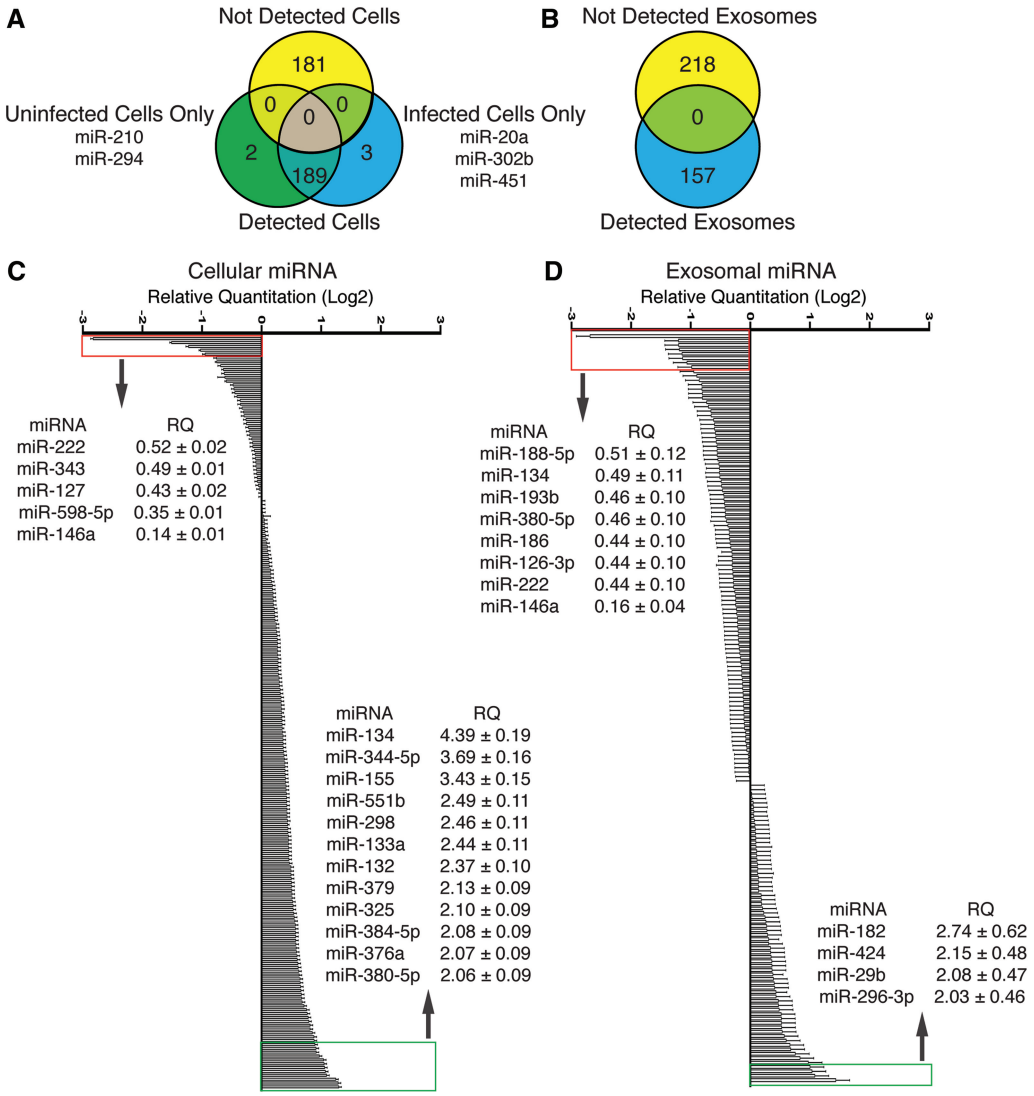

Figure 2. Profiling of miRNA Isolated from prion-infected cells and exosomes. (**A**) Venn diagram of detected miRNA in uninfected and prion-infected cells with TLDA cards that detect 375 known miRNA ($n = 2$). (**B**) Venn diagram of detected miRNA in uninfected and prion-infected exosomes with TLDA cards that detect 375 known miRNA ($n = 2$). (**C**) Relative quantitation of 189 miRNA is detected in uninfected and infected cells. Twelve miRNAs were detected >2-fold up-regulated and five miRNAs were detected as <2-fold down-regulated. Data represent mean ± SEM normalized to sno135 and sno202 endogenous controls using $\Delta\Delta C_t$ method ($n = 2$). (**D**) Relative quantitation of 157 miRNAs detected in uninfected and infected exosomes. Four miRNAs were detected >2-fold up-regulated and eight miRNA were detected as <2-fold down-regulated. Data represent mean ± SEM normalized to sno135 and sno202 endogenous controls using $\Delta\Delta C_t$ method ($n = 2$).

in prion-infected exosomes (Figure 3B). Our candidate miRNA sequences mapped to genomic regions that did not overlap with other annotated transcripts and the flanking sequence folded to form predicted miRNA precursor-like hairpins. However, further work is required to annotate *bona fide* miRNAs from other transcripts among our candidate miRNA sequences, including detection of mature ~22 nt endogenous sequences and Dicer knockdown to confirm that candidates are processed in the miRNA biogenesis pathway.

Together, our results from small RNA sequencing of exosomes demonstrate for the first time that a diverse range of small RNA sequences are packaged within exosomes and the content is not limited to protein, mRNA and miRNAs as previously reported (7).

Known miRNAs sequence reads in prion-infected neuronal exosomes

We observed a range of read counts from 1 to 347 and 1 to 214 that mapped to known miRBase miRNAs in exosomes released from uninfected and prion-infected cells, respectively (Figure 4A). For comparison, the number of reads for a given miRNA was normalized to the total number of miRNA reads in each exosome library, giving the percent normalized read count for each miRNA. Normalization identified miR-29a as the most abundant miRNA in exosomes released from uninfected and prion-infected cells (Figure 4B and Supplementary Table S6). The top 20 most abundant exosome miRNAs included several family members that

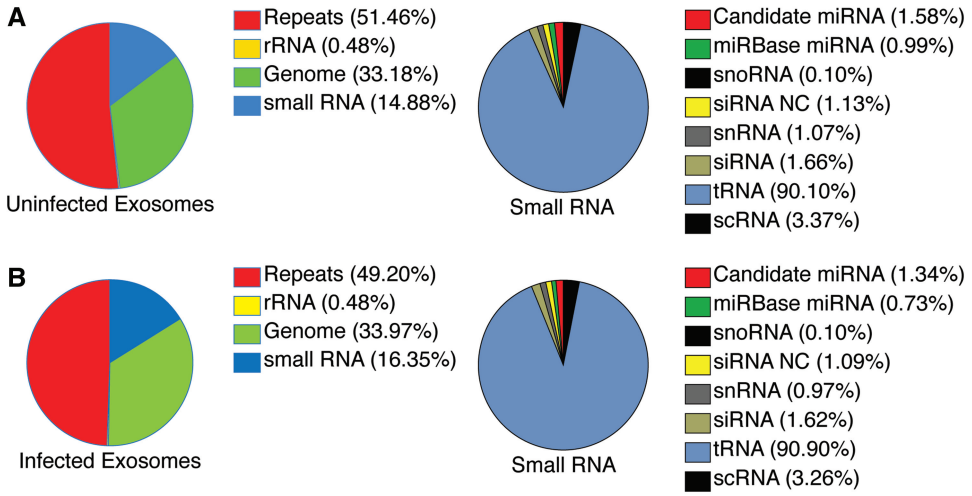

Figure 3. Small RNA library composition from deep sequencing of neuronal exosomes. (**A** and **B**) Percentage reads mapping in uninfected exosome (A) and infected exosome (B) libraries to RNA repeats, rRNA, genomic regions and small RNA. Small RNA mapping is further categorized to tRNA, siRNA and siRNA derived from ncRNA, snoRNA, scRNA, snRNA, mirBase miRNA and candidate miRNA sequences ($n = 2$).

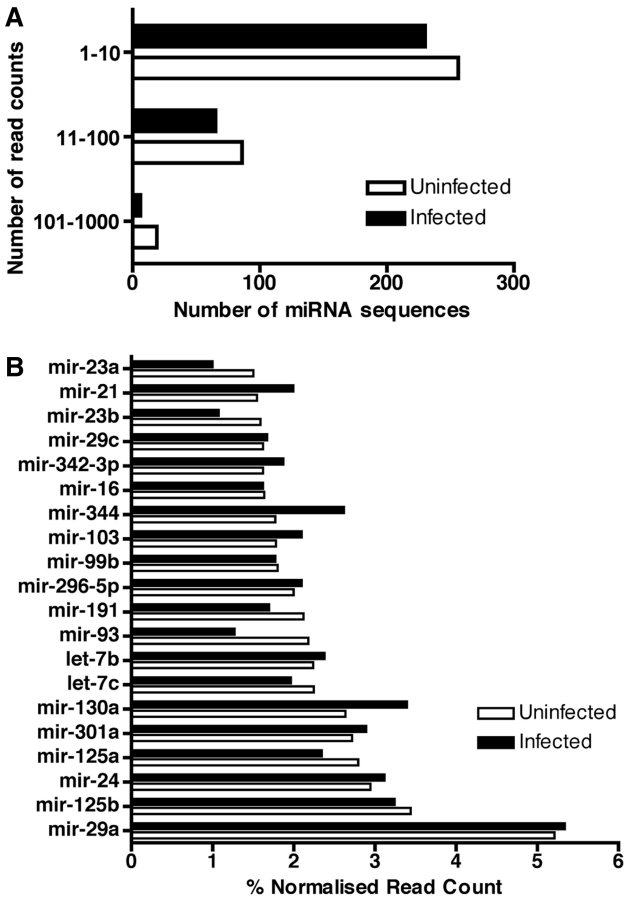

Figure 4. Known miRNAs sequenced in uninfected and prion-infected exosomes. (**A**) Distribution of known miRNA sequences in uninfected and infected exosomes based on the total read counts. Mature miRNA sequences are categorized by number of read counts corresponding to each individual miRNA ($n = 2$). (**B**) Top 20 known miRNAs expressed in uninfected and infected exosomes. The percent contribution of each miRNA sequence in the total pool of known miRNA sequences was calculated by dividing the individual miRNA read count by the total number of known miRNAs sequenced in the corresponding library ($n = 2$).

contain identical seed regions, including let-7 a/7 b/7 c/7i, miR-29 a/29 b/29 c, miR-130 a/130 b/301 a, miR-125 a-5 p/125 b and miR-23 a/23 b families (Figure 4B and Supplementary Table S6). Interestingly, let-7 b and miR-342-3 p, which have previously been shown to be up-regulated in prion-infected brain tissue (17,18), were also identified among the highly represented exosomal miRNAs. Differentially expressed miRNAs were determined by fold change in normalized read counts between uninfected and infected exosome miRNA sequences. let-7i, miR-21, miR-29 b, miR-130 a, miR-344-3 p and miR-378 were all >1.3-fold increased in prion-infected exosomes, while miR-23 a, miR-23 b and miR-93 were all <1.3-fold decreased in prion-infected exosomes (Table 1). It was notable that several miRNA sequences detected using TLDA cards failed to be detected during SOLiD small RNA sequencing. The most significant example we identified was miR-146 a, which failed to be detected in the exosome small RNA libraries, however is significantly down-regulated between uninfected and prion-infected exosomes on TLDA miRNA cards. One possible explanation to this discrepancy is the reported sequencing bias between high-throughput platform technologies and library preparation methods (32,33). Side-by-side Illumina versus SOLiD small RNA sequencing demonstrated that some miRNAs are undetectable on either platform, with several miRNA including miR-146 a not detected by SOLiD small RNA sequencing (33). This underlies the need to validate deep sequencing data with other techniques.

Exosomes released from prion-infected cells contain deregulated miRNAs

To validate known miRNAs that are potentially dysregulated in exosomes isolated from the culture medium of prion-infected neuronal cells, we performed qRT-PCR with specific TaqMan miRNA assays. Due to limitations in the quantity of miRNA within exosomes, we were restricted to the number of miRNA assays that we

Table 1. Differentially detected miRNA from small RNA sequencing of uninfected and infected exosomes

miRNA	Absolute reads uninfected exosomes (*n*)	Absolute reads infected exosomes (*n*)	Normalized uninfected exosomes[a] (%)	Normalized infected exosomes[b] (%)	Infected/ uninfected ratio
miR-130 a	176	136	2.64	3.39	1.30
miR-93	145	51	2.18	1.27	0.58
miR-344-3 p	118	105	1.77	2.62	1.48
miR-23 b	106	43	1.59	1.07	0.67
miR-21	103	80	1.55	2.00	1.30
miR-23 a	100	40	1.50	1.00	0.66
miR-378	82	70	1.23	1.73	1.41
let-7i	58	47	0.87	1.17	1.35
miR-29 b	48	38	0.72	0.95	1.32

[a]Normalized to total number of reads sequenced in pooled uninfected exosomes libraries % 100; $N = 2$; 5939 total reads.
[b]Normalized to total number of reads sequenced in pooled infected exosomes libraries % 100; $N = 2$; 3558 total reads.

Table 2. Summary of dysregulated miRNA 'hits' in exosomes released from prion-infected neuronal cells

Deregulated in miRNA identified in TLDA studies	Highly abundant miRNA identified by SOLiD small RNA sequencing	miRNA dysregulated in prion-infected brain tissue
miR-126-3 p, miR-134, miR-146 a, miR-182, miR-186, miR-188-5 p, miR-193 b, miR-222, miR-296-3 p, miR-29 b, miR-380-5 p and miR-424	let-7 b, **let-7i**, miR-103, miR-125 a-5 p, miR-125 b, **miR-130 a**, miR-130 b, miR-16, **miR-21**, **miR-23 a**, **miR-23 b**, miR-24, miR-296-5 p, miR-29 a, **miR-29 b**, miR-29 c, miR-301 a, miR-30 b, miR-30 c, miR-342-3 p, **miR-344-3 p**, **miR-378** and **miR-93**	let-7 b (17) miR-103 (18) miR-125 a-5 p (17,18) miR-128 a (17,18) miR-146 a (17) miR-342-3 p (17,18)

Highly abundant reads that are >1.3 or <1.3. Differentially detected between uninfected and infected exosomes are indicated in bold. Common miRNAs identified are underlined.

could validate without resorting to pre-amplification techniques that could potentially bias results. Therefore, we carefully selected miRNAs (Table 2) that were dysregulated in our TLDA exosomes miRNA profiling studies (Figure 2B), sequenced in abundance and identified to be differentially expressed in our exosomes small RNA libraries (Table 1 and Supplementary Table S6) or had previously been identified to be deregulated in prion disease. Several miRNAs detected as dysregulated from TLDA miRNA cards (Figure 2B); miR-134, miR-182, miR-193 b and miR-380-5 p were unable to be validated with specific miRNA assay ($C_t > 35$). This is mostly likely due to pre-amplification of cDNA prior to TLDA card analysis introducing potential false positives when cycle threshold detection levels are >30 (Supplementary Table S2).

qRT-PCR miRNA assay of uninfected and prion-infected exosomes identified significantly increased >2-fold miR-21, miR-222 and miR-424 levels; >1.5-fold increases in let-7 b, let-7i, miR-128 a, miR-29 b and miR-342-3 p levels; and <4-fold decreased miR-146 a levels in exosomes released from prion-infected neuronal cells (Figure 5A). While we validated several potential miRNAs (Table 2), miRNAs selected based upon abundance alone failed to show any significant difference in expression between uninfected and prion-infected exosomes, apart from previously identified deregulated miRNAs let-7 b and miR-342-3 p (17,18). Interestingly, both TLDA deregulated miRNAs and differentially detected miRNAs from small RNA sequencing identified 3/9 or 33% and 4/12 or 33% miRNAs significantly dysregulated in prion-infected exosomes, respectively. This would suggest that both methods of miRNA profiling are equally informative in determining miRNA signatures.

To determine if changes observed within exosomes are also present in cells, we performed qRT-PCR miRNA assays on uninfected and prion-infected neuronal cells. In agreement with the exosome data, qRT-PCR validation of miR-146 a was significantly <4-fold decreased in prion-infected cells, while let-7i and miR-21 were significantly >1.5-fold increased in prion-infected cells (Figure 5B). In contrast with our exosome data, miR-23 b was found to be significantly > 2-fold increased in prion-infected cells, while let-7 b, miR-128 a, miR-222, miR-29 b, miR-342-3 p and miR-424 were not significantly altered in expression in prion-infected cells (Figure 5B).

Interestingly, we found some correlation when we compared our validated prion-infected exosomal miRNA signature to previous miRNAs identified in brain tissue from terminally infected prion disease animal models (Supplementary Figure S2). We identified significant increases in let-7 b, let-7i, miR-128 a, miR-21, miR-29 b, miR-222, miR-342-3 p and miR-424, while miR-146 a

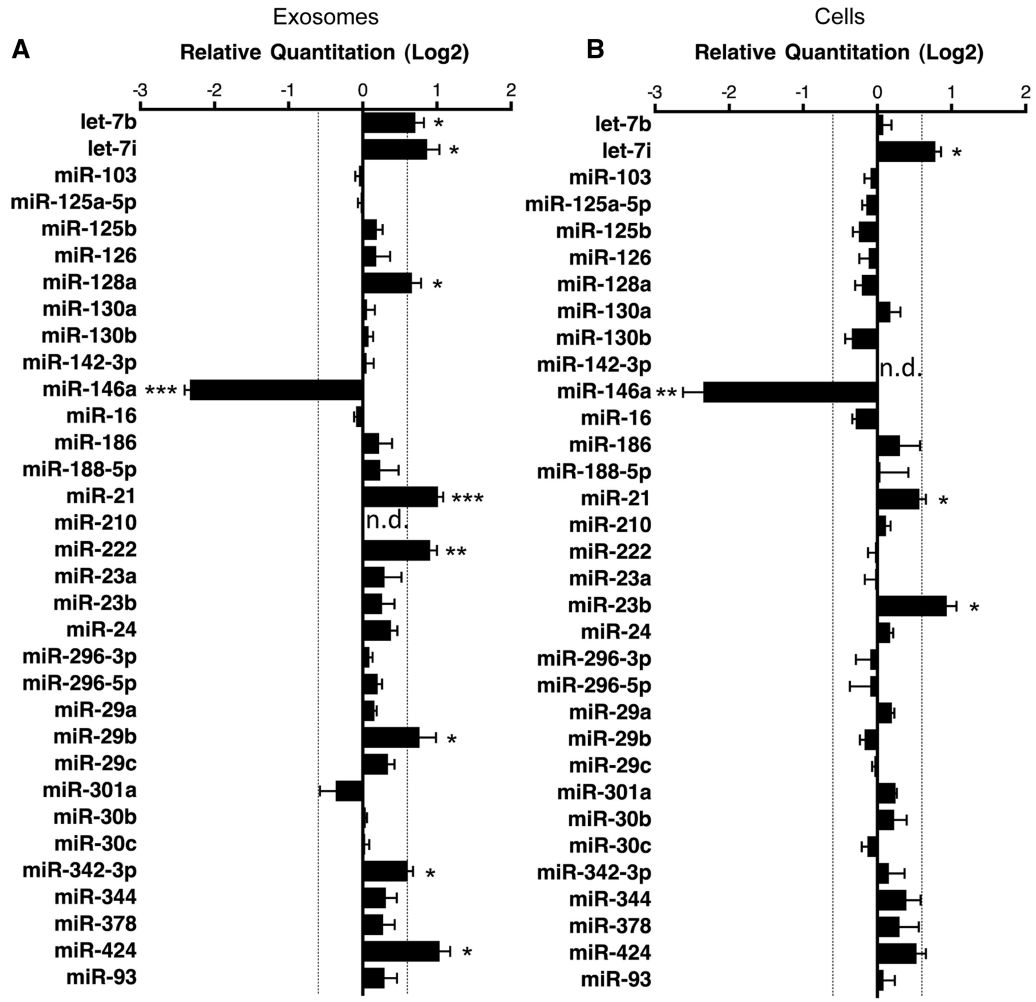

Figure 5. Validation of miRNA 'hits' in infected exosomes and cells. (**A**) Exosomes miRNA detection by TaqMan qPCR miRNA assay, miR-210 was used as a negative control for exosomal miRNA. Relative quantitation data represent mean ± SEM normalized to sno135 and sno202 using $\Delta\Delta C_t$ method. Fold change >1.5 or <1.5 is indicated with significance determined by Mann–Whitney *U*-test; $*P < 0.05$; $**P < 0.01$; $***P < 0.001$ (n = 6–7 independent experiments, n.d. = not detected). (**B**) Cellular miRNA detection by TaqMan qPCR miRNA assay, miR-142-3 p was used as a negative control for cellular miRNA. Relative quantitation data represent mean ± SEM of normalized to sno135 and sno202 using $\Delta\Delta C_t$ method. Fold change >1.5 or <1.5 is indicated by the dashed line with significance determined by Mann–Whitney U-test; $*P < 0.05$; $**P < 0.01$ (n = 6–7 independent experiments, n.d. = not detected).

was significantly decreased in exosomes released from prion-infected neuronal cells. Previously, let-7 b, miR-146 a and miR-128 a were identified as being up-regulated in terminally ill mice infected with prion disease (17), and miR-128 a and miR-342-3 p were identified as being up-regulated in terminally prion-infected primates (18). miR-342-3 p was also identified as being elevated in prion-infected brain regions from human CJD samples (18). Overall, our results support the hypothesis that exosomes released from prion-infected neuronal cells contain a distinct miRNA signature.

DISCUSSION

The cellular prion protein, PrP^{C}, and the infectious form of the prion protein, PrP^{Sc}, have been previously isolated in association with exosomes, with PrP^{Sc} containing exosomes capable of efficiently transmitting infection in both cellular and animal bioassays (4,5,34). This has lead to exosomes being proposed as a mechanism of prion dissemination in an infected host (4,5) and to play a functional role in the spread of neurological disease (6). Exosomes also contain nucleic acid, mRNA and miRNA, which can be functional when transferred between cells (7,8). Circulating exosomes have also been isolated from serum to profile miRNA for diagnosis of diseases such as cancer (14,15,23). Indeed, the existence of a circulating miRNA signature for detecting ovarian cancer from exosomes has been demonstrated. This miRNA signature significantly correlated with primary tumour miRNA expression in women with cancer compared to women with benign disease and was not identified in normal controls (14). Glioblastoma can also be diagnosed by a specific miRNA found to be over-expressed in tumours, and elevated in serum exosomes from patients compared to controls (15). A similarity between miRNA signatures in

circulating exosomal miRNA and originating tumour cells was also found in lung adenocarcinoma, with a significant difference in exosomal miRNA levels between cancer patients and controls (23).

In this study, we determined that exosomes released from prion-infected neuronal cells contain a specific miRNA signature that may be utilized for diagnosis of disease and/or the presence of prion infection. This signature comprises significant up-regulated miRNAs let-7 b, let-7i, miR-128 a, miR-21, miR-222, miR-29 b, miR-342-3 p and miR-424 with down-regulated miR-146 a in exosomes released from prion-infected neuronal cells. These particular miRNAs are deregulated in a variety of cancers, and miRNAs let-7i, miR-128 a, miR-146 a, miR-29 b and miR-424 have been associated with neurological disorders in the miR2Disease database (35). miRNAs let-7i and miR-29 b are down-regulated in sporadic Alzheimer's disease (AD) brains (36), while miR-424 is up-regulated in AD white matter regions (37). Furthermore, miR-128 a is differentially deregulated depending upon the disorder, with up-regulation in AD (36,38) and down-regulation in Huntington's disease (39). miR-146 a has been identified to be up-regulated in AD brains and both murine and human forms of prion disease (17,40–42) and is suggested as a general mechanism of innate immune response and antiviral immunity (41). While these observations are in contrast to our study, increased miR-146 a expression during prion infection is localized to activated microglia cells (40).

Importantly, the deregulated exosomal miRNAs identified in this study correlate with previously reported miRNA changes associated with terminally infected mouse and primate models of prion disease (17,18). Specifically, let-7 b, miR-128 a and miR-342-3 p are significantly up-regulated in terminally prion-infected mouse brains (17), while miR-128 a and miR-342-3 p are significantly up-regulated in brain tissue from primate models infected with BSE prion strains (18). In addition, our results also agree with the reported increase in miR-342-3 p in human brain samples from Type 1 and Type 2 sporadic CJD (18), suggesting that common pathways may be regulated in prion-infected neuronal cells, animal models infected with prion disease and idiopathic forms of prion disease.

Indeed several studies suggest that miRNA present in exosomes can be functionally transferred to recipient cells and activate or repress cellular pathways (7,43–45). Viral miRNAs secreted from infected cells through exosomes have shown to be internalized in recipient cells and functionally repress viral target genes (43). While more recently it was demonstrated that macrophages regulate the invasiveness of breast cancer through exosome-mediated delivery of miRNA into cells promoting metastasis (45). This raises the possibility that transfer of exosomal miRNA from prion-infected cells to uninfected cells may target genes and modulate pathways involved in prion protein propagation and spread of infection. let-7 b, let-7i, miR-128 a, miR-21, miR-222, miR-29 b, miR-342-3 p and miR-424 collectively can target 5916 predicted mRNAs, with 385 experimental validated genes (Supplementary Table S7). Pathway analysis identified several genes that have known interactions with the prion protein including BACE1, SP1, p53, AGO1 and AGO2 (Supplementary Figure S3). miR-29b has been shown to increase the expression of p53 protein (46), while p53 can bind to and increase SP1 promoter binding activity (47). Furthermore, SP1 and p53 transcription factors have both been identified to regulate the expression of the *PRNP* gene (48,49). Since PrP^{C} is explicitly required for prion protein infection (50), deliver of miRNAs in exosomes derived from prion-infected neuronal cells may activate *PRNP* gene expression, therefore stimulating production of PrP^{C} in recipient cells for conversion to PrP^{Sc} and subsequent propagation of infection in the host cell. This supports the mechanism of circulating exosomes in the spread of infection in the host organism. Furthermore, our cellular miRNAs up-regulated during prion infection let-7i, miR-21 and miR-23 b can also increase p53 expression (51), suggesting that activation of *PRNP* gene regulation via p53 expression may be involved in propagation of prion infection. This is supported by observations that p53 knockout mouse cerebellum cells are resistant or have reduced susceptibility to prion infection (52).

Our data also show that the miRNA profile identified in prion-infected exosomes has a remarkably different profile to that of cells (Figure 5A and B), with only let-7i, miR-21 and miR-146 a significantly deregulated in both prion-infected cells and exosomes. By contrast, let-7 b, miR-128 a, miR-222, miR-29 b, miR-342-3 p and miR-424 are up-regulated in exosome released from prion-infected cells, while miR-23 b is up-regulated in prion-infected neuronal cells. This is in agreement with a proposed selective mechanism for the incorporation and release of miRNA in exosomes with several studies demonstrating that exosomes contain little or no 18 S and 28 S cellular ribosomal species; not all mRNA and miRNA contained within cells can be detected in exosomes, and that some mRNA and miRNA can be directly targeted and packaged in exosomes (7,13,14,25,53). These observations suggest that miRNA is selectively incorporated into ILVs as opposed to random events or contamination during the process of exosome isolation.

While the precise mechanism remains unknown, the MVB has been identified as a site for small RNA loading of the RNA-induced silencing complex with GW182 and AGO proteins and miRNA-repressible mRNA transcripts enriched at the MVB (24). Moreover, it was suggested that while miRNA-repressible transcripts are enriched at the MVB, they seem selectively excluded from exosome-like vesicles during ILV formation resulting in under representation of miRNA-repressible mRNAs and enrichment of non-complementary miRNAs being detected in exosomes (24). Comparison of the most abundant mRNA fragments (Supplementary Figure S1B) and the most abundant exosomal miRNA, miR-29 a, (Figure 4B) with its predicted targets suggests that miRNAs are not present in exosomes as a result of binding to complementary 3′-UTR's of target genes. Furthermore, comparison of our significantly up-regulated miRNAs released in exosomes from prion-infected cells and their targets (Supplementary Table S7)

with our abundant exosomal mRNA fragments (Supplementary Figure S1B) also suggest that miRNA:mRNA duplex pairing is an unlikely mechanism of miRNA packaging in exosomes. Remarkably, it has now been shown that PrP^C binds Argonaute proteins AGO1 and AGO2, the essential components of miRNA-induced silencing complexes (miRISCs), at the MVB and promotes formation and stability of miRISCs and miRNA-repressed mRNA transcripts (54). Furthermore, effective repression of several miRNA targets was shown to require expression of PrP^C, directly implicating PrP^C in the miRNA biogenesis pathway. Interestingly, the binding of PrP^C to AGO was facilitated through the octapeptide repeat region of PrP^C (54), with mutations or expansions of this region known to causes familial prion disease (55–57).

While this hypothesis remains to be tested, these observations leave open the possibility that miRNAs are packaged into exosomes as a result of PrP^C binding AGO1 and AGO2 promoting formation of miRISCs on the MVB, which functions as checkpoint for scanning mRNAs. Therefore selecting AGO-bound complementary mRNA:miRNAs that are to be repressed, while non-complementary miRNAs are packaged into ILVs along with PrP^C and released with exosomes. Whether misfolding of PrP^C into PrP^{Sc} during prion disease infection alters its ability to bind to Argonaute proteins, modulates the function of miRISC on the MVB and subsequent release of miRNA in exosomes during prion diseases certainly deserves investigation. Given that, we have identified significant changes in particular miRNA species released in association with exosomes from prion-infected cells, its plausible to suggest that miRNAs are selectively packaged as a direct result of PrP^C and PrP^{Sc} and its influence on the miRNA biogenesis pathway.

In summary, our results strongly support the hypothesis that exosomes released from prion-infected neuronal cells have a distinct miRNA signature that may be utilized for the identification of prion infection. This signature comprises significant increases in let-7 b, let-7i, miR-128 a, miR-21, miR-222, miR-29 b, miR-342-3 p and miR-424 with decreased miR-146 a detection and agrees to some extent to previously reported miRNA changes detected in brains of terminally infected mouse and primate models of prion disease, and sporadic CJD samples (17,18).

Evaluation of our exosomal miRNA signature in circulating exosomes derived from clinical plasma samples from sporadic and variant forms of human prion disease and in animal models infected with different prion strains will be the subject of our further studies. Importantly, it has been shown the miRNAs deregulated in prion-infected exosomes identified in this study have also been detected in circulating exosomes isolated from human serum samples (14), and that neither have currently been detected in disease-associated exosomes in the current literature and a search of ExoCarta database (58), suggesting that this miRNA signature has significant and specific diagnostic potential. However, it should be noted that our study also identified other ncRNAs and mRNA fragments (Supplementary Figure S1) that may also be deregulated in exosomes released from prion-infected neuronal cells. Furthermore, it has been identified that extracellular miRNA released from cells into plasma can associate in two populations, both dependent and independent of exosomes either bound to AGO2 (59–61) or high-density lipoproteins (62). Therefore, targeted exosomal purification strategies for enrichment of circulating miRNA biomarkers may be required to increase biomarker sensitivity (14,15,23). This research also has potential diagnostic implications for other neurodegenerative diseases in which exosomes have been identified to play a role including Alzheimer's disease (63–65), amyotrophic lateral sclerosis (66) and Parkinson's disease (67).

SUPPLEMENTARY DATA

Supplementary Data are available at NAR Online: Supplementary Tables 1–7, Supplementary Figures 1–3, Supplementary Methods and Supplementary References [17–19,22,46–49,51,54,68–71].

ACKNOWLEDGEMENTS

The authors thank Dr Steven Bozinovski (University of Melbourne) for access to 7900-HT instrumentation; Dr Ivonne Petermann, Kelly Ewen-White and John Davis (Life Technologies) for technical assistance with SOLiD library preparation; Sarah Wagner (Molecular and Clinical Pathology Research Laboratory, Clinical and Statewide Services, Queensland Health) for performing the SOLiD sequencing and Dr Eric Hanssen (Bio21 Institute) for assistance with electron microscopy. S.A.B. and A.F.H. designed the research; S.A.B. and B.M.C. performed the research and analysed the data; and S.A.B., B.M.C. and A.F.H. wrote the article.

FUNDING

The National Health Medical Research Council of Australia, in part [567046 Early Career Fellowship to S.A.B.]; Dora Lush Biomedical Postgraduate Scholarship (to B.M.C.); [Program Grant 628946 to A.F.H.]; Australian Research Council [ARC Future Fellowship FT100100560 to A.F.H.]; University of Melbourne Early Career Grant Scheme [600831 Early Career Grant to S.A.B.]. Funding for open access charge: National Health and Medical Research Council.

Conflict of interest statement. None declared.

REFERENCES

1. Prusiner,S.B. (1982) Novel proteinaceous infectious particles cause scrapie. *Science*, **216**, 136–144.
2. Aguzzi,A. and Heikenwalder,M. (2006) Pathogenesis of prion diseases: current status and future outlook. *Nat. Rev. Microbiol.*, **4**, 765–775.
3. Thery,C., Zitvogel,L. and Amigorena,S. (2002) Exosomes: composition, biogenesis and function. *Nat. Rev. Immunol.*, **2**, 569–579.

4. Fevrier,B., Vilette,D., Archer,F., Loew,D., Faigle,W., Vidal,M., Laude,H. and Raposo,G. (2004) Cells release prions in association with exosomes. *Proc. Natl Acad. Sci. USA*, **101**, 9683–9688.
5. Vella,L.J., Sharples,R.A., Lawson,V.A., Masters,C.L., Cappai,R. and Hill,A.F. (2007) Packaging of prions into exosomes is associated with a novel pathway of PrP processing. *J. Pathol.*, **211**, 582–590.
6. Bellingham,S.A., Guo,B.B., Coleman,B.M. and Hill,A.F. (2012) Exosomes: vehicles for the transfer of toxic proteins associated with neurodegenerative diseases? *Front. Physiol.*, **3**, 124.
7. Valadi,H., Ekstrom,K., Bossios,A., Sjostrand,M., Lee,J.J. and Lotvall,J.O. (2007) Exosome-mediated transfer of mRNAs and microRNAs is a novel mechanism of genetic exchange between cells. *Nat. Cell Biol.*, **9**, 654–659.
8. Ratajczak,J., Miekus,K., Kucia,M., Zhang,J., Reca,R., Dvorak,P. and Ratajczak,M.Z. (2006) Embryonic stem cell-derived microvesicles reprogram hematopoietic progenitors: evidence for horizontal transfer of mRNA and protein delivery. *Leukemia*, **20**, 847–856.
9. Bartel,D.P. (2004) MicroRNAs: genomics, biogenesis, mechanism, and function. *Cell*, **116**, 281–297.
10. Vasudevan,S., Tong,Y. and Steitz,J.A. (2007) Switching from repression to activation: microRNAs can up-regulate translation. *Science*, **318**, 1931–1934.
11. Croce,C.M. and Calin,G.A. (2005) miRNAs, cancer, and stem cell division. *Cell*, **122**, 6–7.
12. Esquela-Kerscher,A. and Slack,F.J. (2006) Oncomirs - microRNAs with a role in cancer. *Nat. Rev. Cancer*, **6**, 259–269.
13. Hunter,M.P., Ismail,N., Zhang,X., Aguda,B.D., Lee,E.J., Yu,L., Xiao,T., Schafer,J., Lee,M.L., Schmittgen,T.D. *et al.* (2008) Detection of microRNA expression in human peripheral blood microvesicles. *PLoS One*, **3**, e3694.
14. Taylor,D.D. and Gercel-Taylor,C. (2008) MicroRNA signatures of tumor-derived exosomes as diagnostic biomarkers of ovarian cancer. *Gynecol. Oncol.*, **110**, 13–21.
15. Skog,J., Wurdinger,T., van Rijn,S., Meijer,D.H., Gainche,L., Sena-Esteves,M., Curry,W.T. Jr, Carter,B.S., Krichevsky,A.M. and Breakefield,X.O. (2008) Glioblastoma microvesicles transport RNA and proteins that promote tumour growth and provide diagnostic biomarkers. *Nat. Cell Biol.*, **10**, 1470–1476.
16. Michael,A., Bajracharya,S.D., Yuen,P.S., Zhou,H., Star,R.A., Illei,G.G. and Alevizos,I. (2010) Exosomes from human saliva as a source of microRNA biomarkers. *Oral Dis.*, **16**, 34–38.
17. Saba,R., Goodman,C.D., Huzarewich,R.L., Robertson,C. and Booth,S.A. (2008) A miRNA signature of prion induced neurodegeneration. *PLoS One*, **3**, e3652.
18. Montag,J., Hitt,R., Opitz,L., Schulz-Schaeffer,W.J., Hunsmann,G. and Motzkus,D. (2009) Upregulation of miRNA hsa-miR-342-3 p in experimental and idiopathic prion disease. *Mol. Neurodegener.*, **4**, 36.
19. Kozomara,A. and Griffiths-Jones,S. (2011) miRBase: integrating microRNA annotation and deep-sequencing data. *Nucleic Acids Res.*, **39**, D152–D157.
20. Bu,D., Yu,K., Sun,S., Xie,C., Skogerbo,G., Miao,R., Xiao,H., Liao,Q., Luo,H., Zhao,G. *et al.* (2012) NONCODE v3.0: integrative annotation of long noncoding RNAs. *Nucleic Acids Res.*, **40**, D210–D215.
21. Schatzl,H.M., Laszlo,L., Holtzman,D.M., Tatzelt,J., DeArmond,S.J., Weiner,R.I., Mobley,W.C. and Prusiner,S.B. (1997) A hypothalamic neuronal cell line persistently infected with scrapie prions exhibits apoptosis. *J. Virol.*, **71**, 8821–8831.
22. Tateishi,J., Ohta,M., Koga,M., Sato,Y. and Kuroiwa,Y. (1979) Transmission of chronic spongiform encephalopathy with kuru plaques from humans to small rodents. *Ann. Neurol.*, **5**, 581–584.
23. Rabinowits,G., Gercel-Taylor,C., Day,J.M., Taylor,D.D. and Kloecker,G.H. (2009) Exosomal microRNA: a diagnostic marker for lung cancer. *Clin. Lung Cancer*, **10**, 42–46.
24. Gibbings,D.J., Ciaudo,C., Erhardt,M. and Voinnet,O. (2009) Multivesicular bodies associate with components of miRNA effector complexes and modulate miRNA activity. *Nat. Cell Biol.*, **11**, 1143–1149.
25. Pigati,L., Yaddanapudi,S.C., Iyengar,R., Kim,D.J., Hearn,S.A., Danforth,D., Hastings,M.L. and Duelli,D.M. (2010) Selective release of microRNA species from normal and malignant mammary epithelial cells. *PLoS One*, **5**, e13515.
26. Lu,C., Tej,S.S., Luo,S., Haudenschild,C.D., Meyers,B.C. and Green,P.J. (2005) Elucidation of the small RNA component of the transcriptome. *Science*, **309**, 1567–1569.
27. Sunkar,R., Girke,T., Jain,P.K. and Zhu,J.K. (2005) Cloning and characterization of microRNAs from rice. *Plant Cell*, **17**, 1397–1411.
28. Ruby,J.G., Stark,A., Johnston,W.K., Kellis,M., Bartel,D.P. and Lai,E.C. (2007) Evolution, biogenesis, expression, and target predictions of a substantially expanded set of Drosophila microRNAs. *Genome Res.*, **17**, 1850–1864.
29. Glazov,E.A., Cottee,P.A., Barris,W.C., Moore,R.J., Dalrymple,B.P. and Tizard,M.L. (2008) A microRNA catalog of the developing chicken embryo identified by a deep sequencing approach. *Genome Res.*, **18**, 957–964.
30. Landgraf,P., Rusu,M., Sheridan,R., Sewer,A., Iovino,N., Aravin,A., Pfeffer,S., Rice,A., Kamphorst,A.O., Landthaler,M. *et al.* (2007) A mammalian microRNA expression atlas based on small RNA library sequencing. *Cell*, **129**, 1401–1414.
31. Chiang,H.R., Schoenfeld,L.W., Ruby,J.G., Auyeung,V.C., Spies,N., Baek,D., Johnston,W.K., Russ,C., Luo,S., Babiarz,J.E. *et al.* (2010) Mammalian microRNAs: experimental evaluation of novel and previously annotated genes. *Genes Dev.*, **24**, 992–1009.
32. Linsen,S.E., de Wit,E., Janssens,G., Heater,S., Chapman,L., Parkin,R.K., Fritz,B., Wyman,S.K., de Bruijn,E., Voest,E.E. *et al.* (2009) Limitations and possibilities of small RNA digital gene expression profiling. *Nat. Methods*, **6**, 474–476.
33. Fehniger,T.A., Wylie,T., Germino,E., Leong,J.W., Magrini,V.J., Koul,S., Keppel,C.R., Schneider,S.E., Koboldt,D.C., Sullivan,R.P. *et al.* (2010) Next-generation sequencing identifies the natural killer cell microRNA transcriptome. *Genome Res.*, **20**, 1590–1604.
34. Alais,S., Simoes,S., Baas,D., Lehmann,S., Raposo,G., Darlix,J.L. and Leblanc,P. (2008) Mouse neuroblastoma cells release prion infectivity associated with exosomal vesicles. *Biol. Cell*, **100**, 603–615.
35. Jiang,Q., Wang,Y., Hao,Y., Juan,L., Teng,M., Zhang,X., Li,M., Wang,G. and Liu,Y. (2009) miR2Disease: a manually curated database for microRNA deregulation in human disease. *Nucleic Acids Res.*, **37**, D98–D104.
36. Hebert,S.S., Horre,K., Nicolai,L., Papadopoulou,A.S., Mandemakers,W., Silahtaroglu,A.N., Kauppinen,S., Delacourte,A. and De Strooper,B. (2008) Loss of microRNA cluster miR-29 a/b-1 in sporadic Alzheimer's disease correlates with increased BACE1/beta-secretase expression. *Proc. Natl Acad. Sci. USA*, **105**, 6415–6420.
37. Wang,W.X., Huang,Q., Hu,Y., Stromberg,A.J. and Nelson,P.T. (2011) Patterns of microRNA expression in normal and early Alzheimer's disease human temporal cortex: white matter versus gray matter. *Acta Neuropathol.*, **121**, 193–205.
38. Lukiw,W.J. and Pogue,A.I. (2007) Induction of specific micro RNA (miRNA) species by ROS-generating metal sulfates in primary human brain cells. *J. Inorg. Biochem.*, **101**, 1265–1269.
39. Lee,S.T., Chu,K., Im,W.S., Yoon,H.J., Im,J.Y., Park,J.E., Park,K.H., Jung,K.H., Lee,S.K., Kim,M. *et al.* (2011) Altered microRNA regulation in Huntington's disease models. *Exp. Neurol.*, **227**, 172–179.
40. Saba,R., Gushue,S., Huzarewich,R.L., Manguiat,K., Medina,S., Robertson,C. and Booth,S.A. (2012) MicroRNA 146 a (miR-146 a) is over-expressed during prion disease and modulates the innate immune response and the microglial activation state. *PLoS One*, **7**, e30832.
41. Lukiw,W.J., Dua,P., Pogue,A.I., Eicken,C. and Hill,J.M. (2011) Upregulation of micro RNA-146 a (miRNA-146 a), a marker for inflammatory neurodegeneration, in sporadic Creutzfeldt-Jakob disease (sCJD) and Gerstmann-Straussler-Scheinker (GSS) syndrome. *J. Toxicol. Environ. Health A*, **74**, 1460–1468.
42. Li,Y.Y., Cui,J.G., Hill,J.M., Bhattacharjee,S., Zhao,Y. and Lukiw,W.J. (2011) Increased expression of miRNA-146 a in Alzheimer's disease transgenic mouse models. *Neurosci. Lett.*, **487**, 94–98.
43. Pegtel,D.M., Cosmopoulos,K., Thorley-Lawson,D.A., van Eijndhoven,M.A., Hopmans,E.S., Lindenberg,J.L., de Gruijl,T.D., Wurdinger,T. and Middeldorp,J.M. (2010) Functional delivery of

viral miRNAs via exosomes. *Proc. Natl Acad. Sci. USA*, **107**, 6328–6333.
44. Kosaka,N., Iguchi,H., Yoshioka,Y., Takeshita,F., Matsuki,Y. and Ochiya,T. (2010) Secretory mechanisms and intercellular transfer of microRNAs in living cells. *J. Biol. Chem.*, **285**, 17442–17452.
45. Yang,M., Chen,J., Su,F., Yu,B., Lin,L., Liu,Y., Huang,J.D. and Song,E. (2011) Microvesicles secreted by macrophages shuttle invasion-potentiating microRNAs into breast cancer cells. *Mol. Cancer*, **10**, 117.
46. Feng,Z., Zhang,C., Wu,R. and Hu,W. (2011) Tumor suppressor p53 meets microRNAs. *J. Mol. Cell Biol.*, **3**, 44–50.
47. Amini,S., Saunders,M., Kelley,K., Khalili,K. and Sawaya,B.E. (2004) Interplay between HIV-1 Vpr and Sp1 modulates p21(WAF1) gene expression in human astrocytes. *J. Biol. Chem.*, **279**, 46046–46056.
48. Bellingham,S.A., Coleman,L.A., Masters,C.L., Camakaris,J. and Hill,A.F. (2009) Regulation of prion gene expression by transcription factors SP1 and metal transcription factor-1. *J. Biol. Chem.*, **284**, 1291–1301.
49. Vincent,B., Sunyach,C., Orzechowski,H.D., St George-Hyslop,P. and Checler,F. (2009) p53-dependent transcriptional control of cellular prion by presenilins. *J. Neurosci.*, **29**, 6752–6760.
50. Bueler,H., Aguzzi,A., Sailer,A., Greiner,R.A., Autenried,P., Aguet,M. and Weissmann,C. (1993) Mice devoid of PrP are resistant to scrapie. *Cell*, **73**, 1339–1347.
51. Tarasov,V., Jung,P., Verdoodt,B., Lodygin,D., Epanchintsev,A., Menssen,A., Meister,G. and Hermeking,H. (2007) Differential regulation of microRNAs by p53 revealed by massively parallel sequencing: miR-34a is a p53 target that induces apoptosis and G1-arrest. *Cell Cycle*, **6**, 1586–1593.
52. Mays,C.E., Kang,H.E., Kim,Y., Shim,S.H., Bang,J.E., Woo,H.J., Cho,Y.H., Kim,J.B. and Ryou,C. (2008) CRBL cells: establishment, characterization and susceptibility to prion infection. *Brain Res.*, **1208**, 170–180.
53. Montecalvo,A., Larregina,A.T., Shufesky,W.J., Beer Stolz,D., Sullivan,M.L., Karlsson,J.M., Baty,C.J., Gibson,G.A., Erdos,G., Wang,Z. *et al.* (2012) Mechanism of transfer of functional microRNAs between mouse dendritic cells via exosomes. *Blood*, **119**, 756–766.
54. Gibbings,D., Leblanc,P., Jay,F., Pontier,D., Michel,F., Schwab,Y., Alais,S., Lagrange,T. and Voinnet,O. (2012) Human prion protein binds Argonaute and promotes accumulation of microRNA effector complexes. *Nat. Struct. Mol. Biol.*, **19**, 517–524.
55. Owen,F., Poulter,M., Lofthouse,R., Collinge,J., Crow,T.J., Risby,D., Baker,H.F., Ridley,R.M., Hsiao,K. and Prusiner,S.B. (1989) Insertion in prion protein gene in familial Creutzfeldt-Jakob disease. *Lancet*, **1**, 51–52.
56. Owen,F., Poulter,M., Shah,T., Collinge,J., Lofthouse,R., Baker,H., Ridley,R., McVey,J. and Crow,T.J. (1990) An in-frame insertion in the prion protein gene in familial Creutzfeldt-Jakob disease. *Brain Res. Mol. Brain Res.*, **7**, 273–276.
57. Goldfarb,L.G., Brown,P., McCombie,W.R., Goldgaber,D., Swergold,G.D., Wills,P.R., Cervenakova,L., Baron,H., Gibbs,C.J. Jr and Gajdusek,D.C. (1991) Transmissible familial Creutzfeldt-Jakob disease associated with five, seven, and eight extra octapeptide coding repeats in the PRNP gene. *Proc. Natl Acad. Sci. USA*, **88**, 10926–10930.
58. Mathivanan,S., Fahner,C.J., Reid,G.E. and Simpson,R.J. (2012) ExoCarta 2012: database of exosomal proteins, RNA and lipids. *Nucleic Acids Res.*, **40**, D1241–D1244.
59. Arroyo,J.D., Chevillet,J.R., Kroh,E.M., Ruf,I.K., Pritchard,C.C., Gibson,D.F., Mitchell,P.S., Bennett,C.F., Pogosova-Agadjanyan,E.L., Stirewalt,D.L. *et al.* (2011) Argonaute2 complexes carry a population of circulating microRNAs independent of vesicles in human plasma. *Proc. Natl Acad. Sci. USA*, **108**, 5003–5008.
60. Turchinovich,A., Weiz,L., Langheinz,A. and Burwinkel,B. (2011) Characterization of extracellular circulating microRNA. *Nucleic Acids Res.*, **39**, 7223–7233.
61. Gallo,A., Tandon,M., Alevizos,I. and Illei,G.G. (2012) The majority of microRNAs detectable in serum and saliva is concentrated in exosomes. *PLoS One*, **7**, e30679.
62. Vickers,K.C., Palmisano,B.T., Shoucri,B.M., Shamburek,R.D. and Remaley,A.T. (2011) MicroRNAs are transported in plasma and delivered to recipient cells by high-density lipoproteins. *Nat. Cell Biol.*, **13**, 423–433.
63. Rajendran,L., Honsho,M., Zahn,T.R., Keller,P., Geiger,K.D., Verkade,P. and Simons,K. (2006) Alzheimer's disease beta-amyloid peptides are released in association with exosomes. *Proc. Natl Acad. Sci. USA*, **103**, 11172–11177.
64. Sharples,R.A., Vella,L.J., Nisbet,R.M., Naylor,R., Perez,K., Barnham,K.J., Masters,C.L. and Hill,A.F. (2008) Inhibition of gamma-secretase causes increased secretion of amyloid precursor protein C-terminal fragments in association with exosomes. *FASEB J.*, **22**, 1469–1478.
65. Saman,S., Kim,W., Raya,M., Visnick,Y., Miro,S., Jackson,B., McKee,A.C., Alvarez,V.E., Lee,N.C. and Hall,G.F. (2012) Exosome-associated tau is secreted in tauopathy models and is selectively phosphorylated in cerebrospinal fluid (CSF) in early Alzheimer's Disease. *J. Biol. Chem.*, **287**, 3842–3849.
66. Gomes,C., Keller,S., Altevogt,P. and Costa,J. (2007) Evidence for secretion of Cu,Zn superoxide dismutase via exosomes from a cell model of amyotrophic lateral sclerosis. *Neurosci. Lett.*, **428**, 43–46.
67. Emmanouilidou,E., Melachroinou,K., Roumeliotis,T., Garbis,S.D., Ntzouni,M., Margaritis,L.H., Stefanis,L. and Vekrellis,K. (2010) Cell-produced alpha-synuclein is secreted in a calcium-dependent manner by exosomes and impacts neuronal survival. *J. Neurosci.*, **30**, 6838–6851.